Walking droplets in a Faraday-Talbot corral

N. Sungar,* J. P. Sharpe, M. Duce, M. Niesyt, and S. Hopfe
Department of Physics, Cal Poly, San Luis Obispo, California 93407, USA

(Received 8 September 2020; accepted 13 May 2021; published 26 May 2021)

Previous studies have demonstrated that the complex motion of a droplet moving on a vibrated fluid surface can yield a long-term statistical behavior reminiscent of that of quantum particles. This is especially the case when the droplet is confined within a small corral. Here we investigate the motion of walkers in a large corral with the boundary constructed from a circular array of pillars that protrude through the fluid surface. Our measurements demonstrate that the structure of the corral walls affects the droplet position probability distribution.

DOI: 10.1103/PhysRevFluids.6.053604

I. INTRODUCTION

When a millimeter-sized droplet of oil is placed on a vibrated bath of the same oil, the drop can bounce indefinitely, sustained by a film of air that does not drain during the contact between the droplet and the fluid surface. As it bounces, the droplet generates a wave on the surface that propagates away from the point of impact. When the droplet returns to the bath, it thus lands on a surface that is shaped by the waves due to the previous impacts. If the vibration acceleration is increased further, the droplet can start to move parallel to the fluid surface, becoming what is called a "walker." This is the result of horizontal transfer of momentum from the waves to the droplet, and it is these waves that determine the horizontal motion of the droplet and how it interacts with other droplets and boundaries [1–3].

Coupling between the particle and an underlying wavefield is a situation analogous to the pilot-wave theory in quantum mechanics, and over the past decade many studies have explored the behavior of these walking droplets [4–8]. A recent review [9] summarizes the current state of the field.

Of particular interest here is the effect of the bath boundaries on the motion of the droplets, with an obvious analogy to the well-known quantum system of a particle-in-a-box. In a seminal study [10], it was demonstrated that the long-term behavior of a droplet in a circular bath mimicked the behavior of an electron in a quantum corral. Although the short-term motion of the droplet appeared to be complex and disordered, when the motion was averaged over a long time the probability distribution of the droplet position revealed circular regions of high and low probability. It was found that this distribution corresponded with the amplitude of the linear Faraday wave mode of the corral.

A physical wall is not the only way of obtaining a closed-system quantum analog. In Refs. [11,12], confinement of the droplet was obtained by spinning the entire vibrating liquid bath so that the droplet experienced a central inward force due to the deformation of the fluid surface. Perrard *et al.* [13] applied a central inward force by embedding a small drop of ferrofluid within the droplet and using a local magnetic field. In Ref. [14], not only was the vibrating fluid contained within a small elliptical cavity, but the topography of the bath bottom was also varied to create an

*nsungar@calpoly.edu

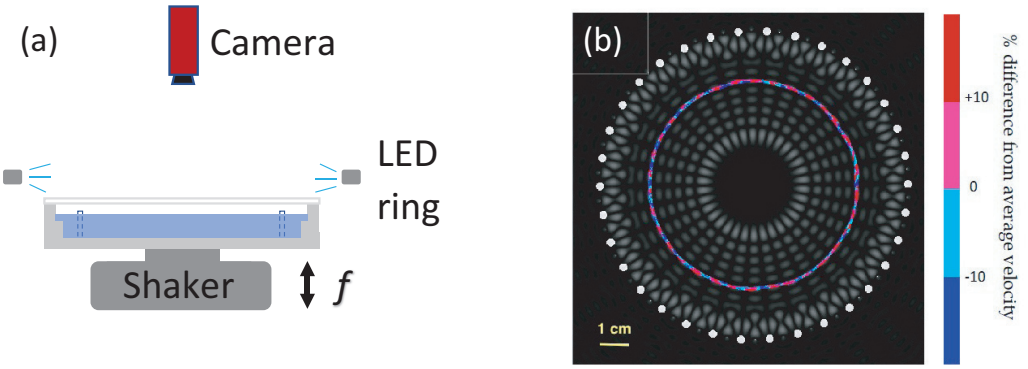

FIG. 1. (a) Side view of shaker and oil tray. The tray has a circular pillar corral, which in turn is surrounded by raised beaches to suppress wave reflection from outer boundaries. The tray is covered with an acrylic lid to prevent air currents, and the droplets on the fluid surface are illuminated from the side using a ring of white-light LEDs. A camera directly above the tray records the drop motion. (b) Trajectory of a 0.63-mm-diam drop when the bath is driven at $f = 55$ Hz at an acceleration $\gamma = 0.99\gamma_F$. Data obtained from 30 min of video recording. The circular trajectory of the drop has a radius of 40.3 mm and is color-coded to show the percentage difference of its speed from the average speed. The trajectory is superimposed on a simulated Faraday-Talbot intensity pattern where bright regions correspond to fluid displacement antinodes and dark regions to nodes. This pattern would be observed if the acceleration was above the Faraday threshold.

analog of the quantum "mirage." In all these systems, quantization of the trajectories of the droplet were observed.

In this paper, we study the motion of droplets constrained to move in a bath where the circumference of the bath is not a solid wall but is composed of a circular array of small plastic pillars that protrude through the surface of the fluid. When driven at just the right frequency and a high enough amplitude, this arrangement gives rise to Faraday waves that are organized as if the waves had originated from point sources located between the pillars [15,16]. The resultant near-field interference pattern, which is an eigenmode of the fluid surface, is referred to as the Faraday-Talbot pattern [17]. We find that if the bath is vibrated with sufficient acceleration to support walkers, but is still below the Faraday threshold, then the droplet behaves in a fashion that reflects the underlying symmetries of the above-threshold Faraday mode. We demonstrate that engineering the corral wall, hence imposing a specific Faraday mode, influences the droplet position probability distribution.

We report measurements of the motion of a fixed-size droplet just below the Faraday threshold. We find that the motion of the drop is strongly correlated with the intensity of the wave field that would occur if the fluid were accelerated above the Faraday threshold. We identify three distinct regimes of increasingly complex motion as the Faraday threshold is approached: circular orbits, meandering motion about an orbit, and complex motion with looping and changes in direction. In the next section, we briefly describe the experimental arrangement, and then we examine these regimes in detail.

II. EXPERIMENTAL ARRANGEMENT

The experimental setup is sketched in Fig. 1(a). It consists of a 16-cm-diam circular bath containing silicone oil that is oscillated vertically at a frequency $f = 55$ Hz with an electromagnetic shaker. The oil, which has a viscosity of 20 cS, fills the bath to a height of $h = 6.0 \pm 0.5$ mm. A shallow "beach" region of width 10 mm at the edge of the bath serves to dampen the waves at the boundary. The acceleration $\gamma(t) = \gamma_0 \cos(2\pi f t)$, where $\gamma_0 = 4\pi^2 f^2 A$ is controlled by varying the vibration amplitude A. The oscillation of the shaker is monitored by two accelerometers mounted on opposite sides of the bath, and a feedback system to the amplifier driving the shaker maintains

the acceleration to within about $0.005g$, where g is the acceleration due to gravity. Within the bath, a circular, periodic array of 34 pillars, each with diameter 3.18 ± 0.01 mm and separated by a center-to-center distance $d = 11$ mm, protrudes from the oil surface. This spacing corresponds to $d \sim 1.5\lambda_F$, where λ_F is the Faraday wavelength at the driving frequency of 55 Hz. With this setup, when the acceleration is ~0.5–1 % above the Faraday threshold γ_F, a stable Faraday-Talbot pattern [16] is produced on the surface and oscillates at half the driving frequency.

Droplets of the same silicone oil with diameter 0.63 ± 0.01 mm were generated with a piezoelectric droplet-on-demand generator [18] and dropped onto the vibrating fluid surface. The acceleration was kept just under the Faraday threshold ($\sim 0.990\gamma_F$–$0.998\gamma_F$). Air currents that may affect the drop's motion in the bath were eliminated by sealing the bath with an acrylic lid. A circular LED strip above the bath provided uniform lighting almost parallel to the fluid surface such that the motion of the drop could be tracked using an in-house particle-tracking algorithm written in MATLAB. All particle-tracking videos reported here were recorded at 20 frames/s at a resolution of 750×750 pixels with a CCD camera.

III. EXPERIMENTAL RESULTS

We first summarize our observations and then describe in more detail the different regimes of drop behavior.

When the bath is shaken at 55 Hz, the Faraday threshold acceleration is measured to be $\gamma_F = 2.230 \pm 0.005g$. At this frequency, the drop does not start walking until an acceleration of $0.98\gamma_F$ is reached. In this walking regime, we observe that the vertical bouncing mode of the drop is (2,2) [19]. At the onset of walking the motion is very slow, with droplets moving at 1–2 mm/s, along almost straight paths when near the center of the bath and curved paths when closer to the pillars. As the acceleration is increased, the drop settles into a circular orbit at a radius of 36.5 mm, with an average speed of 2.5 mm/s. When the acceleration is again increased and approaches $0.99\gamma_F$, the drop reaches an average speed of 3.7 mm/s and settles into a different circular orbit, one at a radius of 40.3 mm and thus closer to the pillars. As the acceleration is increased further, the average speed of the drop does not change significantly, but it moves even closer to the pillars and starts meandering along a circular path. At $0.998\gamma_F$, the drop's motion becomes even more irregular, featuring stops, changes in direction, and small loops. When the acceleration reaches γ_F, the Faraday-Talbot pattern appears on the surface and the drop gets trapped around the peaks of the pattern.

In general, the drop's speed changes along its trajectory, and since these variations in speed occur on spatial scales comparable to those of the above-threshold Faraday pattern, the droplet trajectories are superimposed on a computer-generated image of the intensity of the Faraday-Talbot pattern. This image is obtained by modeling the Faraday-Talbot standing-wave pattern as a fluid-surface displacement field arising from point sources located between the pillars [15,16]. We plot the intensity pattern, which is the square of the amplitude of the fluid surface displacement. The image can be seen in Fig. 1(b), where the bright regions are antinodes of the fluid oscillation, and the dark regions are nodes.

In the next sections, we present observations and analysis of drop motion in three different regimes as the acceleration is increased. We are specifically interested in any correlation between the motion and the underlying Faraday-Talbot intensity pattern, which is the resonant Faraday mode for the bath configuration. To characterize the behavior of the drop, we count the number of times the drop visits each pixel over the course of the video to create a histogram, and we also measure the drop speed by measuring the change in position between frames.

A. Circular motion

For the lowest accelerations at which the drop moves, two different stable circular orbits were observed. The inner orbit is at a radius of 36.5 mm and is stable at accelerations $0.985\gamma_F$–$0.990\gamma_F$,

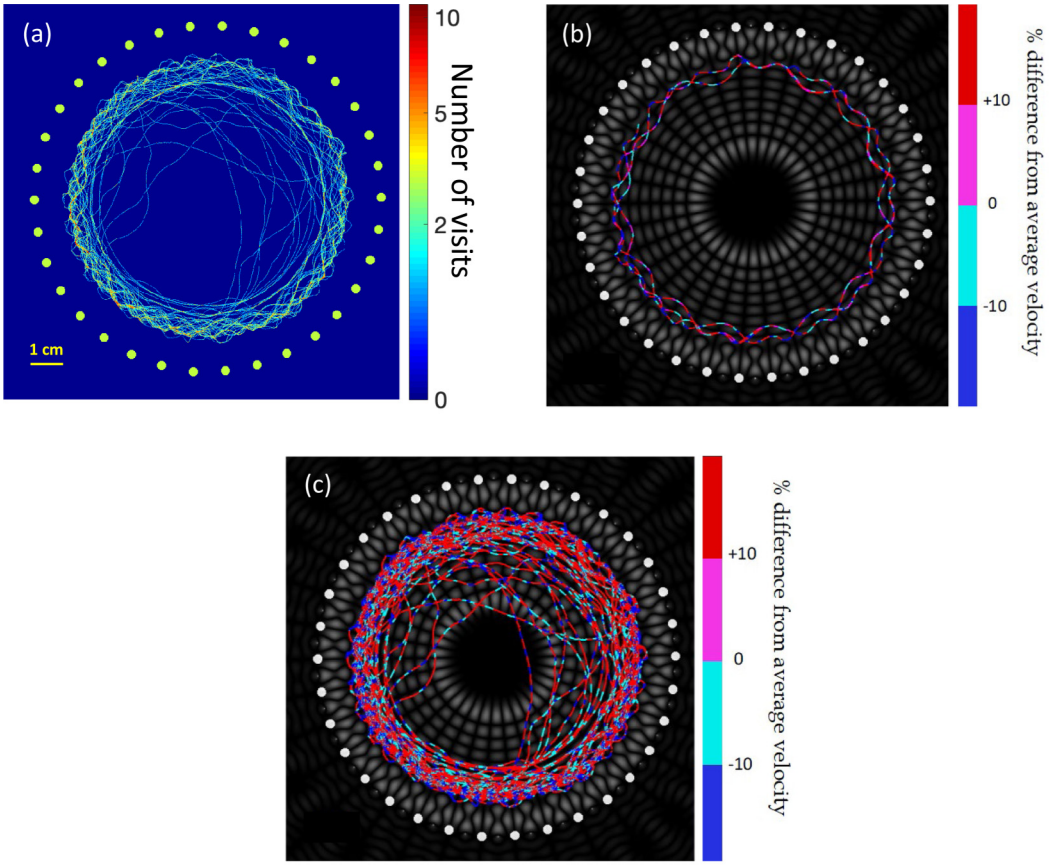

FIG. 2. (a) Droplet position histogram obtained from ∼60 min of recordings when the bath is driven at $f = 55$ Hz at an acceleration $0.995\gamma_F$. Each pixel is color-coded to show the number of times the drop visited that pixel. (b) A sample drop trajectory (5 min of recording) superimposed on a simulated Faraday-Talbot intensity pattern. The trajectory is color-coded to show the percentage difference of the drop's speed from the average speed. (c) Drop trajectories obtained from ∼60 min of recordings, color-coded as in (b).

where the drop is moving at an average speed of 2.5 mm/s. The radius of this orbit corresponds to one of the rings of antinodes of the intensity pattern

The outer orbit is at a radius of 40.3 mm and is stable at accelerations $0.990\gamma_F$–$0.995\gamma_F$, where the drop is moving at an average speed of 3.7 mm/s. The position of the orbit again coincides with a ring of antinodes of the Faraday-Talbot intensity pattern. This can be seen in Fig. 1(b), where we computed at each pixel visited by the drop the difference between the instantaneous speed and the average speed, and we color-coded the path to show speeds above and below average. We find that the drop's speed is strongly correlated with the pattern, and it is above average passing through antinodal positions and below average passing through nodal positions.

Quantized circular orbits have also been observed in previous studies [10–13,20]. In small corrals [10,20], circular orbits appear such that the radii correspond to the maxima of the cavity mode of the corral. In other studies [11–13], circular orbits are induced by imposing an external central force either through rotation of the bath or by magnetic forces. At lower memory the orbit radius can be changed continuously by changing the central force. As the vibration acceleration is increased and the path memory becomes significant, only orbits with specific radii are found to be stable, leading to quantization of orbits. This quantization is explained by the appearance of an additional radial

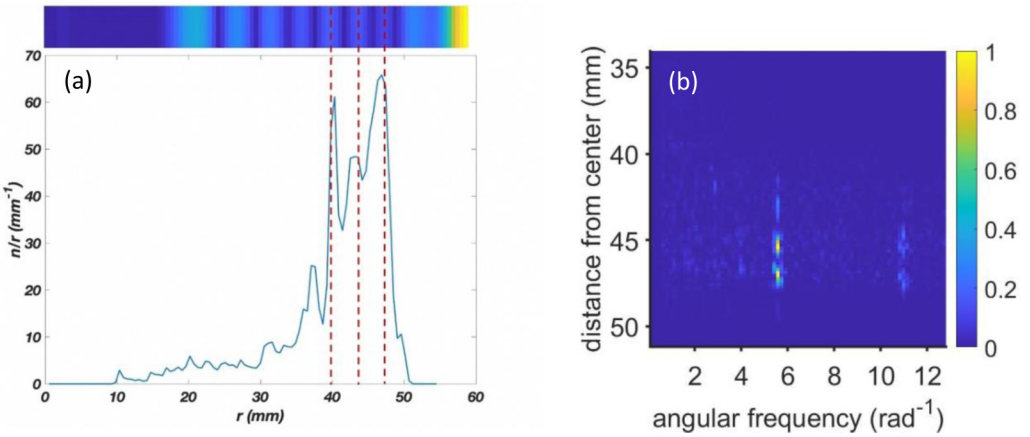

FIG. 3. (a) Radial histogram of droplet position (solid line), where n/r is the number of visits per mm the drop makes at radius r. The color bar at the top indicates the positions of nodes (darker regions) and antinodes (lighter regions) of the Faraday-Talbot pattern in the radial direction. The bath is driven at $f = 55$ Hz at an acceleration $0.995\gamma_F$. (b) Angular power spectrum of position histogram as a function of radial distance from the center of the bath. The power spectral density has been arbitrarily scaled to 1 at its maximum.

force as a result of long path memory. When waves resulting from previous impacts of the drop along the whole orbit contribute, the surface slope at the drop's position has a radial component. This produces a radial force on the drop in addition to the external central force. Only for specific radii does this transverse component of the surface slope become zero, stabilizing the orbit and yielding the observed quantization.

We infer that a similar mechanism produces the circular orbits in our system. Since we have no external central force, the circular orbits we see are induced by the boundaries made of pillars. Without the pillars, walkers travel in a straight line. The fluid in the interpillar spaces becomes excited by the walker as it passes near them, and it produces waves that spread across the surface. For specific radii, superposition of these waves results in a radial force on the walker that is just right to provide the centripetal force for a stable orbit at that radius. The fact that stable orbits only coincide with radii where one would see a Faraday-Talbot ring of antinodes (and thus the same phase relationship among the waves) when the fluid is driven above threshold lends credence to this idea.

B. Meandering and partially circular motion

At $0.995\gamma_F$, the drop can start meandering and move closer to the pillars, though it can also transition back and forth between this meandering motion and the circular orbit at 40.3 mm radius.

Figure 2(a) shows the droplet position histogram obtained from an hour of recording. Meandering and circular structures can be clearly discerned. Figure 2(b) has a small sample of the motion showing both the droplet position and speed, where we have again color-coded the trajectory to indicate the locations where the speed is above or below the average.

We have also superimposed the trajectory on the computer-generated image of the Faraday-Talbot intensity pattern. The drop position and speed vary on a spatial scale commensurate with that of the above-threshold pattern, and the droplet generally moves faster (red) in the vicinity of the antinodes and slower (blue) when at the nodes. Figure 2(c) shows a much longer trajectory, also color-coded to represent the relative speed of the drop.

Since the Faraday-Talbot pattern has variations in both radial and angular directions, we utilize two different methods to pick out the characteristics of the motion in these directions: a radial histogram and a spectral decomposition of the position variations in the azimuthal direction. To

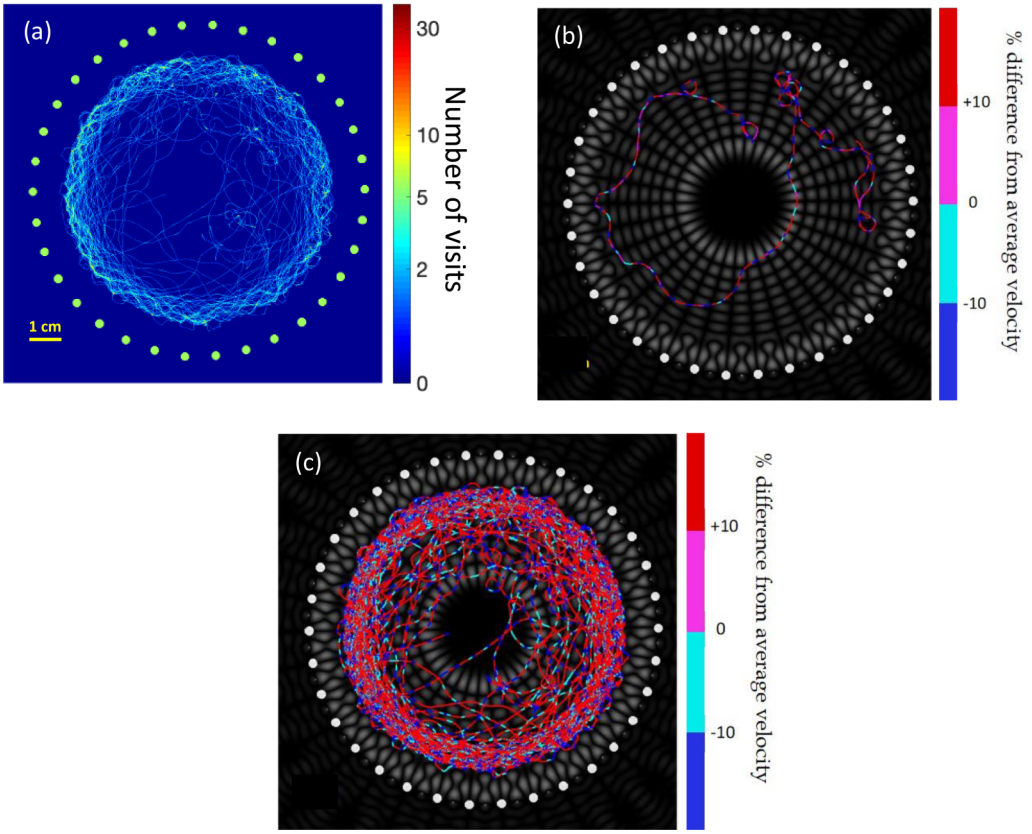

FIG. 4. (a) Droplet position histogram obtained from ∼90 min of recordings when the bath is driven at $f = 55$ Hz at an acceleration $0.998\gamma_F$. Each pixel is color-coded to show the number of times the drop visited that pixel. (b) A sample of the trajectory of the droplet (2 min recording) color-coded to show relative speed. (c) Droplet trajectories obtained from ∼90 min of recordings, color-coded as in part (b).

construct the histogram in the radial direction, at each radius we integrate the position histogram in the azimuthal direction to obtain n, the number of times the drop visited radius r. Then we divide n by the radius to obtain a spatial density at that radius. To detect variations in motion that are present in the angular direction, we extract rings from the position histogram at each radius and calculate their power spectra. If the long-term statistical behavior of the drop shows a signature of the underlying resonant mode, which has a 34-fold symmetry, it should have peaks at an angular frequency of $34/2\pi$ rad^{-1}.

Figure 3(a) shows how the radial histogram is related to the radial intensity pattern of the underlying wave field. At radius $r = 40.3$ mm, a maximum of the radial histogram coincides almost exactly with the position of an antinode, where a circular orbit was observed. At $r = 43$ and 46.7 mm there are also maxima that are aligned with the Faraday-Talbot antinodes, but these are slightly off-centered. Figure 3(b) shows the power spectrum of the histogram in the angular direction as a function of radial distance. Strong peaks occur in the spectrum at an angular frequency of $34/2\pi$ rad^{-1}, showing that the droplet position exhibits variations with the same periodicity as the pillar array, which is the same azimuthal periodicity of the underlying Faraday-Talbot pattern. The two most prominent peaks occur at radii of 45.5 and 47 mm. These radii straddle the radial position of the histogram maximum and Faraday-Talbot antinode at 46.7 mm seen in Fig. 3(a), and they are due to the meandering motion of the walker. The fact that the peaks in the spectrum are at specific

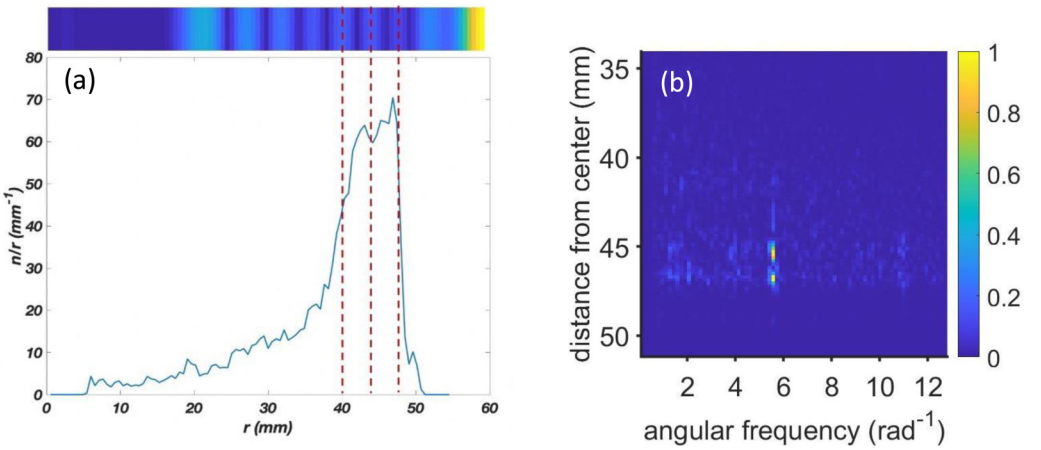

FIG. 5. (a) Radial histogram of droplet position (solid line), where n/r is the number of times per mm the droplet visited radius r. The color bar at the top indicates the positions of nodes (darker regions) and antinodes (lighter regions) of the Faraday-Talbot pattern in the radial direction when the bath is driven at $f = 55$ Hz at an acceleration $0.998\gamma_F$. (b) Angular power spectrum of position histogram as a function of radial distance. The power spectral density has been arbitrarily scaled to 1 at its maximum.

radii that straddle an antinodal ring of the Faraday-Talbot pattern is evidence that the droplet is influenced by the eigenmode of the corral.

C. Looping and reversing motion

As the acceleration reaches $0.998\gamma_F$, the droplet's motion becomes more erratic, involving changes in direction and small loops, and it explores a greater area on the surface, as shown by the histogram in Fig. 4(a). In this regime, the motion is similar to the random-walk-like jittering motion described in Ref. [21]. Figure 4(b) shows a short sample of trajectory illustrating the looping and reversing motion, while Fig. 4(c) shows a much longer trajectory color-coded to represent the relative speed of motion.

Now the trajectories are more complicated and the motion appears almost random. As can be seen from the radial histogram in Fig. 5(a), the drop localizes in the regions where the peaks were present at lower memory, but the peaks are now indistinguishable. The power spectrum of the position histogram in the angular direction [Fig. 5(b)] shows clear peaks at a spatial frequency of $34/2\pi$ rad^{-1} and at the same radial distances discussed under the meandering motion. The small loops seen in Fig. 4(b) are at the scale of the intensity pattern, and they are located around an antinode or around the spot where nodal lines would cross if the fluid were driven above threshold. At these highest accelerations, we observed that the droplet bounces chaotically. In experiments with smaller corrals [10,14,20], at high memory where the dynamics of the drop is chaotic, the long-term statistics is prescribed by the Faraday mode of the cavity. However, in our experiment, in this regime, although the power spectrum shows some evidence of the underlying wavefield, the peaks in the radial histogram become indistinct.

IV. DISCUSSION

The emergence of a wavelike statistical behavior in hydrodynamic quantum analogs in the high memory regime has been observed in both closed systems, such as small corrals [10,14,20], and open systems [22], where a submerged well in the fluid acts as a scattering center for the droplet. In both cases, it has been determined that the oscillations or variations in droplet speed induced by the wave field play an important role in the long-term statistical behavior of the droplet.

The experiments reported here involve a larger corral that has a unique eigenmode with variations in both radial and angular directions. The experiments exhibit two significant features of the statistical behavior of droplets that are seen in hydrodynamic quantum analogs. The first feature is the variation in the speed of the droplet induced by interactions of the pilot wave with boundaries, and the second is the correlation of the long-time statistics of the droplet's motion with the Faraday modes of the system. Three different regimes of behavior are observed as the acceleration is increased from $0.990\gamma_F$ to $0.998\gamma_F$. At lower accelerations, when the droplet is in a circular orbit, the speed variation is periodic with the periodicity of the array. Around $0.995\gamma_F$ we see a meandering motion that is well correlated with the underlying wavefield. At the highest accelerations, the motion of the droplet is jittery and random-walk-like. In all regimes, the droplet speed varies at the scale of the Faraday wavelength. It may be noted that although the wave excitations due to the droplet do not fill the entire corral at any one time, the long-time statistics of the droplet motion reflect the underlying structure of the supra-threshold Faraday-Talbot pattern.

The observations reported here are consistent with a recently developed theoretical treatment of an idealized hydrodynamic pilot wave system [21]. There it was shown that small perturbations can lead to speed oscillations, and that periodic or chaotic jittering motion emerges at sufficiently high memory. This provides a rationale for the observed statistical structures in experiments where the boundary influences the motion of the droplet, and it suggests that similar statistical behavior should be observed in a broad class of hydrodynamic systems.

ACKNOWLEDGMENTS

The authors thank the Bill and Linda Frost Fund for support of this work, and the anonymous referees for the many useful comments, which greatly improved this paper.

[1] Y. Couder, S. Protière, E. Fort, and A. Boudaoud, Walking and orbiting droplets, Nature **437**, 208 (2005).
[2] S. Protière, A. Boudaoud, and Y. Couder, Particle wave association on a fluid interface, J. Fluid. Mech. **554**, 85 (2006).
[3] A. Eddi, E. Sultan, J. Moukhtar, E. Fort, M. Rossi, and Y. Couder, Information stored in Faraday waves: The origin of a path memory, J. Fluid Mech. **674**, 433 (2011).
[4] Y. Couder and E. Fort, Single-Particle Diffraction and Interference at a Macroscopic Scale, Phys. Rev. Lett. **97**, 154101 (2006).
[5] G. Pucci, P. J. Sáenz, L. Faria, and J. W. M. Bush, Non-specular reflection of walking droplets, J. Fluid Mech. **804**, 1 (2016).
[6] G. Pucci, D. M. Harris, L. Faria, and J. W. M. Bush, Walking droplets interacting with single and double slits, J. Fluid Mech. **835**, 1136 (2017).
[7] D. M. Harris, P.-T. Brun, A. Damiano, L. Faria, and J. W. M. Bush, The interaction of a walking droplet and a submerged pillar: From scattering to the logarithmic spiral, Chaos **28**, 096105 (2018).
[8] J. W. M. Bush, Pilot-wave hydrodynamics, Annu. Rev. Fluid Mech. **47**, 269 (2015).
[9] J. W. M. Bush and A. U. Oza, Hydrodynamic quantum analogs, Rep. Prog. Phys. **84**, 017001 (2021).
[10] D. M. Harris, J. Moukhtar, E. Fort, Y. Couder, and J. W. M. Bush, Wavelike statistics from pilot-wave dynamics in a circular corral, Phys. Rev. E **88**, 011001(R) (2013).
[11] E. Fort, A. Eddi, A. Boudaoud, J. Moukhtar, and Y. Couder, Path-memory induced quantization of classical orbits, Proc. Natl. Acad. Sci. USA **107**, 17515 (2010).
[12] D. M. Harris and J. W. M. Bush, Droplets walking in a rotating frame: From quantized orbits to multimodal statistics, J. Fluid Mech. **739**, 444 (2014).
[13] S. Perrard, M. Labousse, M. Miskin, E. Fort, and Y. Couder, Self-organization into quantized eigenstates of a classical wave-driven particle, Nat. Commun. **5**, 3219 (2014).
[14] P. J. Sáenz, T. Cristea-Platon, and J. W. M. Bush, Statistical projection effects in a hydrodynamic pilot-wave system, Nat. Phys. **14**, 315 (2017).

[15] N. Sungar, L. D. Tambasco, G. Pucci, P. J. Sáenz, and J. W. M. Bush, Hydrodynamic analog of particle trapping with the Talbot effect, Phys. Rev. Fluids **2**, 103602 (2017).
[16] N. Sungar, J. P. Sharpe, J. J. Pilgram, J. Bernard, and L. D. Tambasco, Faraday-Talbot effect: Alternating phase and circular arrays, Chaos **28**, 096101 (2018).
[17] K. Patorski, The self-imaging phenomenon and its applications, Progr. Opt. **27**, 1 (1989).
[18] D. M. Harris, L. Tanya, and J. W. M. Bush, A low-cost, precise piezoelectric droplet-on-demand generator, Exp. Fluids **56**, 83 (2015).
[19] J. Molácek and J. W. M. Bush, Drops bouncing on a vibrating bath, J. Fluid Mech. **727**, 582 (2013).
[20] T. Cristea-Platon, P. J. Sáenz, and J. W. M. Bush, Walking droplets in a circular corral: Quantization and chaos, Chaos **28**, 096116 (2018).
[21] M. Durey, S. E. Turton, and J. W. M. Bush, Speed oscillations in classical pilot-wave dynamics, Proc. R. Soc. A **476**, 20190884 (2020).
[22] P. J. Sáenz, T. Cristea-Platon, and J. W. M. Bush, A hydrodynamic analog of Friedel oscillations, Sci. Adv. **6**, eaay9234 (2020).